Journal of Applied Polymer Science

Effects of thermal treatment on the CO_2 sorption of triblockcopolymers derived from polyimide and poly(methylmethacrylate)

Shota Ando, Akihiro Yoshida, Kazukiyo Nagai
Department of Applied Chemistry, Meiji University, Kawasaki 214-8571, Japan
Correspondence to K. Nagai (E-mail: nagai@meiji.ac.jp)

ABSTRACT: ABA-type triblock copolymers were synthesized using 4,4-(hexafluoroisopropylidene) diphthalic anhydride-2,3,5,6-tetramethyl-1,4-phenylenediamine (6FDA-TeMPD) and poly(methyl methacrylate) (PMMA). The films were characterized by determining the effects of different content ratios and thermal decomposition of PMMA block on CO_2 sorption properties. TGA results showed that a thermal labile block can be completely decomposed under a previously reported thermal condition. SEM results presented that the asperity was micro-phase separation caused by the PMMA block content rate. Numerous pores with sizes of approximately 10 to 50 nm were detected on Block(28/72) and Block(10/90). The isotherms of all films fitted the dual-mode sorption model, and CO_2 sorption decreased with increased PMMA content rate. Infinite-dilution CO_2 solubility depended on the Langmuir's site of each polymer because S_{H0}/S_0 of PI and Block(PI/PMMA) varied from 0.84 to 0.92 CO_2 affinity was increased by thermal treatment as indicated by the higher b and S_0 values of thermally treated films than those of nontreated films. © 2015 Wiley Periodicals, Inc. J. Appl. Polym. Sci. **2015**, *132*, 42208.

KEYWORDS: copolymers; degradation; films; polyimides; radical polymerization

Received 23 January 2015; accepted 16 March 2015
DOI: 10.1002/app.42208

INTRODUCTION

Aromatic polyimides are widely used as structural, electronic, and optical materials because of their good thermal stability, mechanical strength, and optical properties.[1–4] In particular, fluorine-containing polyimides, such as 4,4-hexafluoroisopropylidene diphthalic anhydride (6FDA)-based polyimides, exhibit higher gas permeability and CO_2 selectivity than other polyimides because they contain trifluoromethyl group. 6FDA-based polyimides containing 2,3,5,6-tetramethyl-1,4-phenylene diamine (TeMPD) have been applied for optical materials,[5,6] electronic materials,[7,8] molecularly oriented liquid-crystal films,[9,10] and gas/vapor separation materials.[11–15] Recently, thermal treatment has gained attention for improving highly functional polyimides because it can control primary and film structures. For example, thermal rearrangement induces polymers to form a suitable structure through cleavage and recombination of chemical bonds.[16–21] During carbonization, the organic components of polymers are converted into inorganic components through thermal treatment and restructuring of primary structure. Moreover, polymer chains are rearranged through heating at temperature higher than T_g and under slow cooling during annealing. Porous formation is a process in which the pores in films are introduced through thermal decomposition of the polymer chains.[22] Several reported show that block copolymers chemically coupled with aromatic polyimides and thermally labile polymers, such as poly(methyl methacrylate) (PMMA), poly(propylene oxide), and poly(ethylene glycol). Thermal labile blocks can be selectively decomposed to obtain high functionalization because of their easy molecular design and properties of thermal labile block, including dielectric property, light weight, and gas permeability.[7,23–27] We have reported the synthesis of ABA-type triblock copolymers by using fluorine-containing polyimides and PMMA with different composition ratios; these polymers can increase the dielectric constant through thermal treatment and control water vapor concentration,[7,27–29] while there are no studies on the CO_2 sorption property of thermal-treated block copolymer derived from Polyimide and PMMA. This study reported the effects of PMMA content and thermal treatment on CO_2 sorption of ABA-type triblock copolymers derived from 6FDA-TeMPD (PI) and PMMA.

EXPERIMENTAL

Film Preparation

PI, PMMA, and triblock copolymer have been used to synthesize a sample in previous study.[29] The chemical structure and composition ratio of these polymers are shown in Figure 1 and

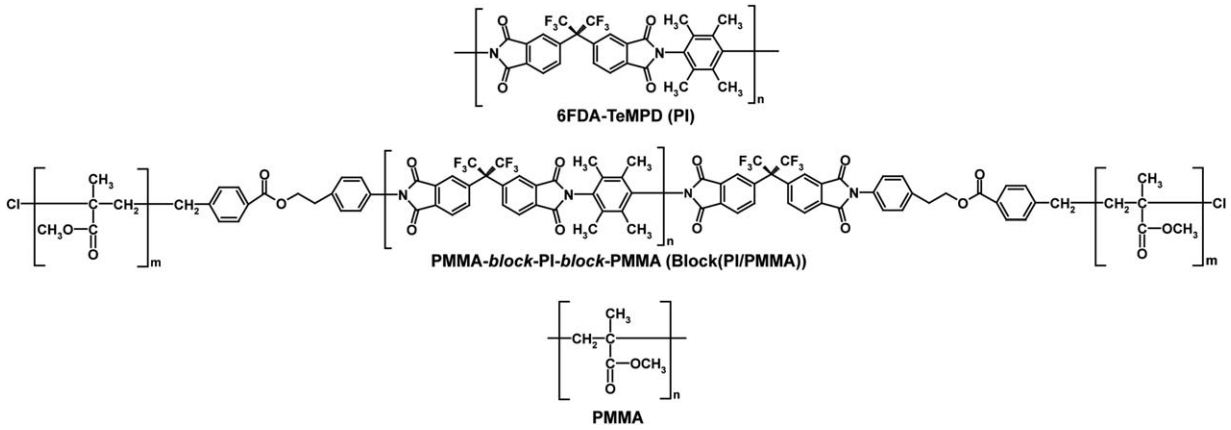

Figure 1. Chemical structures of PI, PMMA, and PMMA-block-PI-block-PMMA (Block(PI/PMMA)).

Table I. Similar to previous study,[29] films were prepared on a Teflon petri dish by casting 3 wt % chloroform solution to obtain a film thickness of 100 to 140 μm. The plate was covered with a glass dish to decrease the rate of solvent evaporation and prevent contamination in atmospheric pressure at 23 ± 1°C. The solvent was allowed to evaporate for 72 h. The solvent was removed by placing in a methanol solution at 23 ± 1°C for 1 week. The films were dried at 100°C for 12 h to remove the solvent. All experiments were performed on the dried film with a thickness difference of ± 1 μm.

Thermal Analysis

The films were analyzed using a Pyris 1 thermogravimetric analyzer (TGA, PerkinElmer Inc., Shelton). About 1.0 mg of the polymer sample was heated from 50 to 300°C in a platinum pan at a heating rate of 30°C/min and flow rate of 60 mL/min in air atmosphere. The polymer sample was then heated at a constant temperature of 300°C for 12 h. Complete decomposition was observed in PMMA block of the block copolymer.

Glass-transition temperature (T_g) was determined using a diamond differential scanning calorimeter (PerkinElmer Inc.). DSC measurements were performed at 50°C to 200°C with a heating rate of 10°C/min in nitrogen atmosphere before pyrolysis. A natural cooling condition was adopted. About 10 mg of the polymer sample was placed in aluminum sample pan kit. T_g was determined from the first and second heating scan and set as the middle point of the endothermic transition. All measured data were obtained in the film state. A minimum of three samples were analyzed to confirm the reproducibility of the experimental results.

Structure and Analysis

Film density (ρ) was measured with flotation method at 23 ± 1°C by using calcium nitrate tetrahydrate (Junsei Chemical Co. Ltd., Tokyo, Japan).

Fourier transform-infrared spectrometry (FT-IR) spectroscopy with KBr method at 23 ± 1°C was performed using an FT/IR-4100 (Jasco Co., Tokyo, Japan). Each spectrum was determined from 32 scans at a resolution of 2 cm^{-1} and then averaged.

Scanning electron microscopy (SEM) was performed with a high-resolution field-emission SEM (FE-SEM) (S5200, Hitachi High-Technologies Corporation, Tokyo, Japan). SEM sample was prepared by surface coating with a magnetron-type ion-sputtering instrument (JCS-1600, JEOL, Ltd., Tokyo, Japan). The sample was coated with platinum at 70 s and 30 mA. Acceleration voltage of SEM was 5 kV.

All measurement data were obtained in the film state. A minimum of three samples were used to confirm the reproducibility of the experimental results.

Table I. PMMA Content of 6FDA-TeMPD (PI), PMMA, and Block(PI/PMMA)

	PMMA content					T_g (PMMA block) (°C)		ΔC_p(PMMA block) (J/(g K))	
Polymer	NMR[a] (mol %)	NMR[a] (wt %)	NMR (vol %)	TGA (wt %)	TGA isotherms (wt %)	1st scan	2nd scan	1st scan	2nd scan
PI	0	0	0	0	0	N/A	N/A	N/A	N/A
Block (73/27)	27	6	5	7	7	N/A	N/A	N/A	N/A
Block (28/72)	72	31	32	27	31	135 ± 1	143 ± 1	2.413 ± 0.240	0.058 ± 0.005
Block (10/90)	90	60	62	55	60	135 ± 1	124 ± 1	3.154 ± 1.194	0.369 ± 0.132
PMMA	100	100	100	100	-	135 ± 1	113 ± 2	3.310 ± 0.538	0.392 ± 0.059

[a] Cited from Ref. 29.

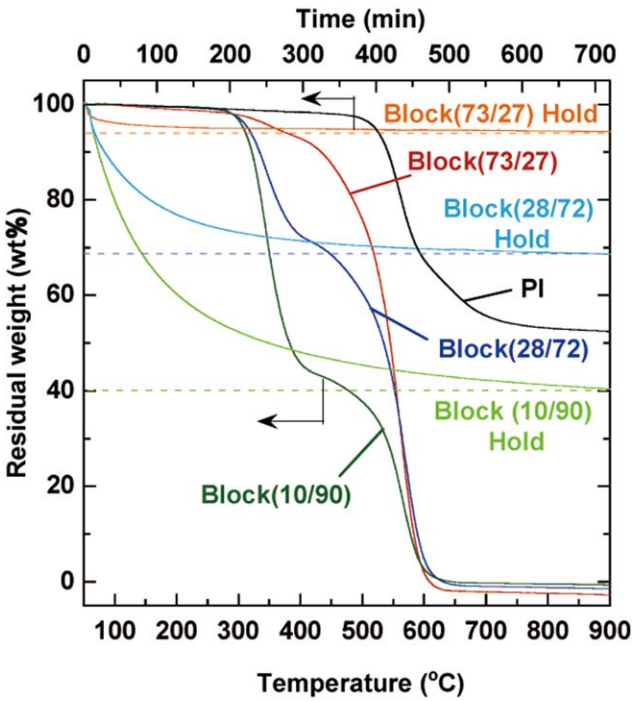

Figure 2. TGA curves and isotherms of Block(PI/PMMA) in air atmosphere. [Color figure can be viewed in the online issue, which is available at wileyonlinelibrary.com.]

CO_2 Sorption

The equilibrium sorption isotherm of pure CO_2 in all films was volumetrically determined as a function of pressure at 35°C by using a pressure–decay system. The sample was introduced into the chamber to degas the polymer film, and the sorption system was left overnight at 35°C. Pure CO_2 was introduced into the sorption chamber. Penetrant uptake was recorded up to 50 atm as a function of time. All measurement data were obtained in the film state. A minimum of three samples were analyzed to confirm the reproducibility of the experimental results.

RESULTS AND DISCUSSION

Thermal Analysis

The result of increasing the temperature in a previous study[29] is shown in Figure 2. Two thermal decomposition steps were observed in Block(PI/PMMA) and the decomposition weight of each step corresponded to the composition ratio of each block. This finding suggested that decomposition products of the first and second steps were PMMA and polyimide blocks, respectively. The complete decomposition of the PMMA block from Block(PI/PMMA) was confirmed with the TGA isotherm reported in a previous study.[7] Therefore, we also used this condition for the present investigation.

Figure 2 presents the TGA decomposition curves and isotherms in a previous study.[7] The TGA isotherms at 300°C of triblock copolymer showed that the residual weight of PMMA block gradually decreased for 12 h. After 12 h, the residual weights of Block(73/27), Block(28/72), and Block(10/90) were 93, 69, and 40 wt %, respectively; these values included weight ratios of TGA in ± 1%. Therefore, the PMMA block in Block(PI/PMMA) can be completely decomposed at 300°C for 12 h in air atmosphere.

Figure 3 presents the DSC curves of each polymer. T_g of 6FDA-TeMPD was 422°C at one peak. Few small and narrow thermal transformations were observed in PMMA and Block(PI/PMMA), and T_g was the thermal transformation with the highest specific heat capacity. The T_g values of PMMA, Block(10/90), and Block(28/72) were 135°C in the first scan and 113°C, 124°C, and 143°C, respectively, in the second scan. T_g of Block(73/27) was 200°C and was not observed in the first and second scans. The T_g values of PMMA, Block(10/90), and Block(28/72) in the first scan indicated that the unrelaxed state of the PMMA block in Block(PI/PMMA) was similar to that of PMMA homopolymer. Moreover, the T_g values of PMMA and

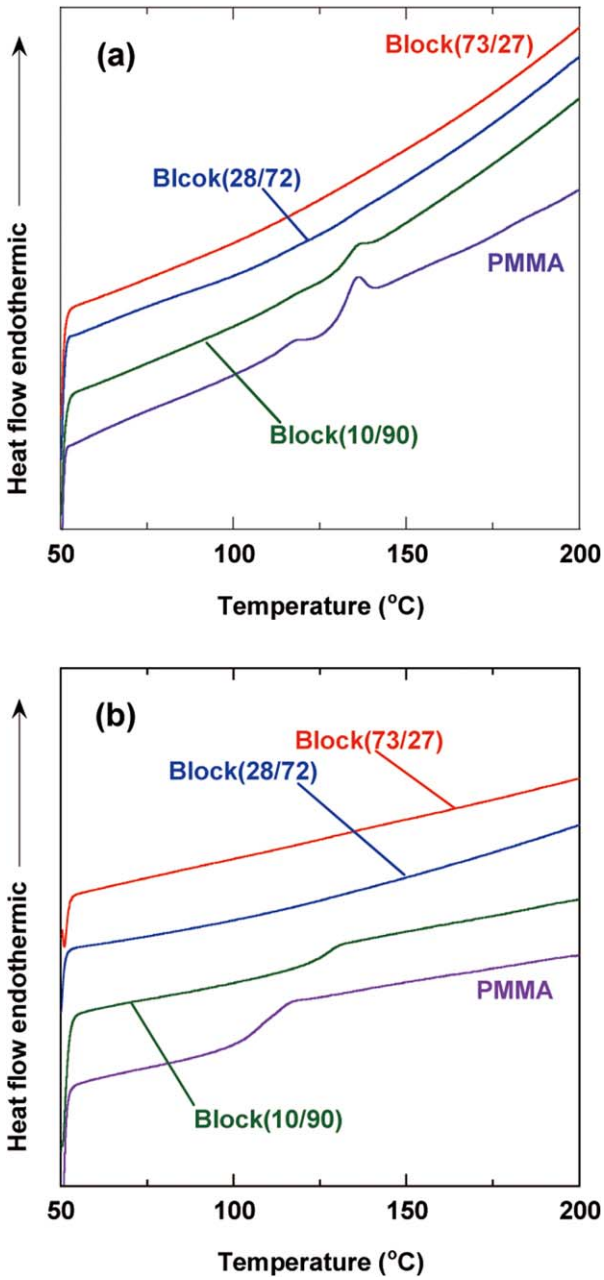

Figure 3. DSC curves of Block(PI/PMMA) in nitrogen atmosphere; (a) first scan and (b) second scan. [Color figure can be viewed in the online issue, which is available at wileyonlinelibrary.com.]

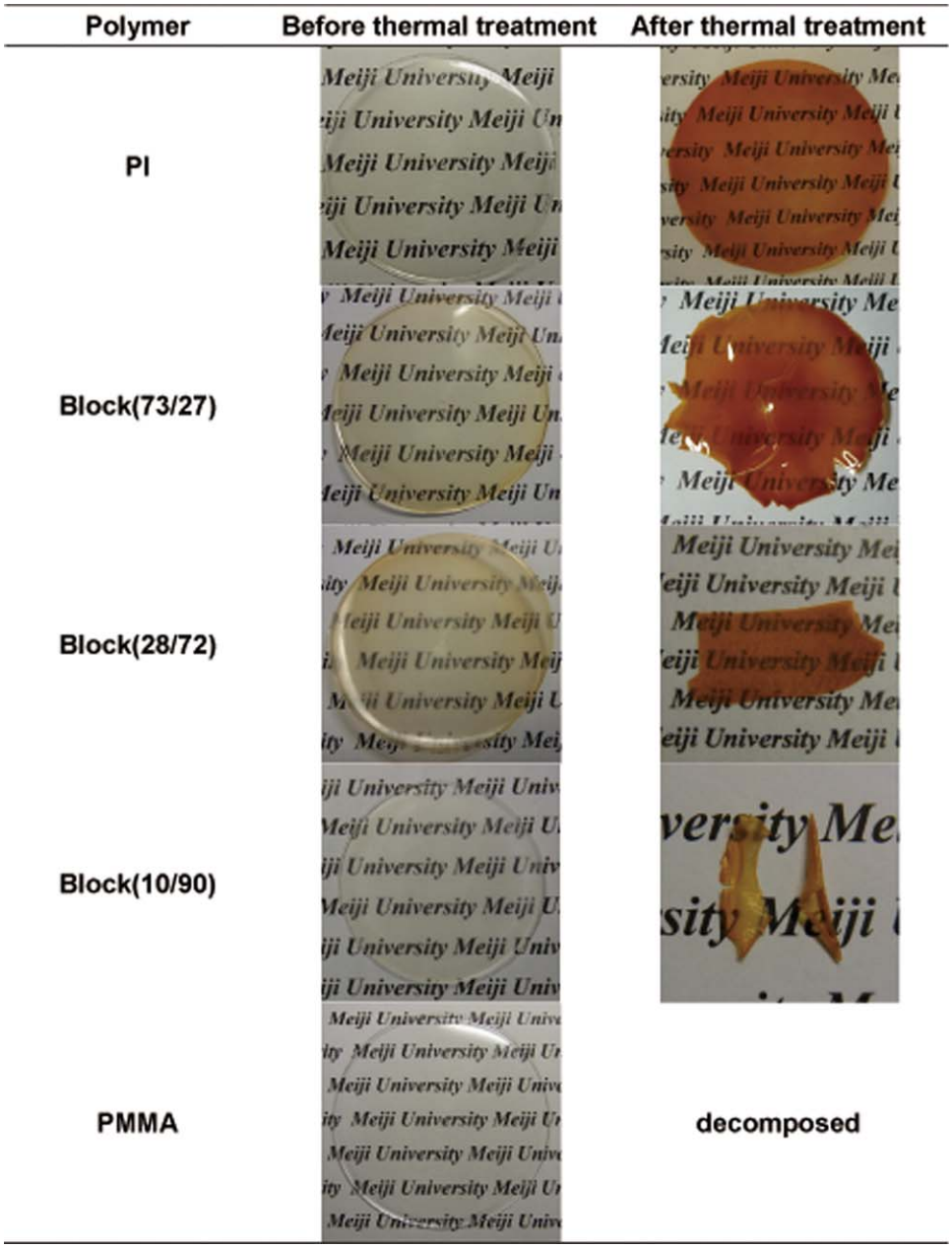

Figure 4. Photoimages of Block(PI/PMMA) films. [Color figure can be viewed in the online issue, which is available at wileyonlinelibrary.com.]

Block(PI/PMMA) in the second scan increased with decreasing PMMA content. These results suggested that triblock copolymer with shorter PMMA block was significantly affected compared with the copolymer with longer PMMA blocks and PMMA.

Thermal Treatment of Block Copolymer

Thermally treated films were prepared under a heating condition presented in previous study.[7] The films were heated to induce thermal degradation of decomposition component (PMMA block). The treatment condition included 150°C for 1 h, 200°C for 1 h, 240°C for 1 h in vacuum atmosphere, and 300°C for 12 h in air atmosphere.

Figure 4 presents the photo images of each polymer film before and after thermal treatment. All thermally treated films were clear and brown, and the film strength decreased with increasing PMMA content. Block(10/90), which comprised 70% of the weight ratio of PMMA, could not maintain the film shape through decomposition using thermal treatment because this block contained large mass of PMMA. Thermally treated films were not dissolved in *N*,*N*-dimethylformamide, tetrahydrofran, and chloroform but were soluble before thermal treatment. Therefore, solvent solubility resistance of thermally treated films was higher than that of the nontreated films.

Figure 5 presents the FT-IR spectra of each polymer before and after thermal treatment. As PMMA increased, the peaks around

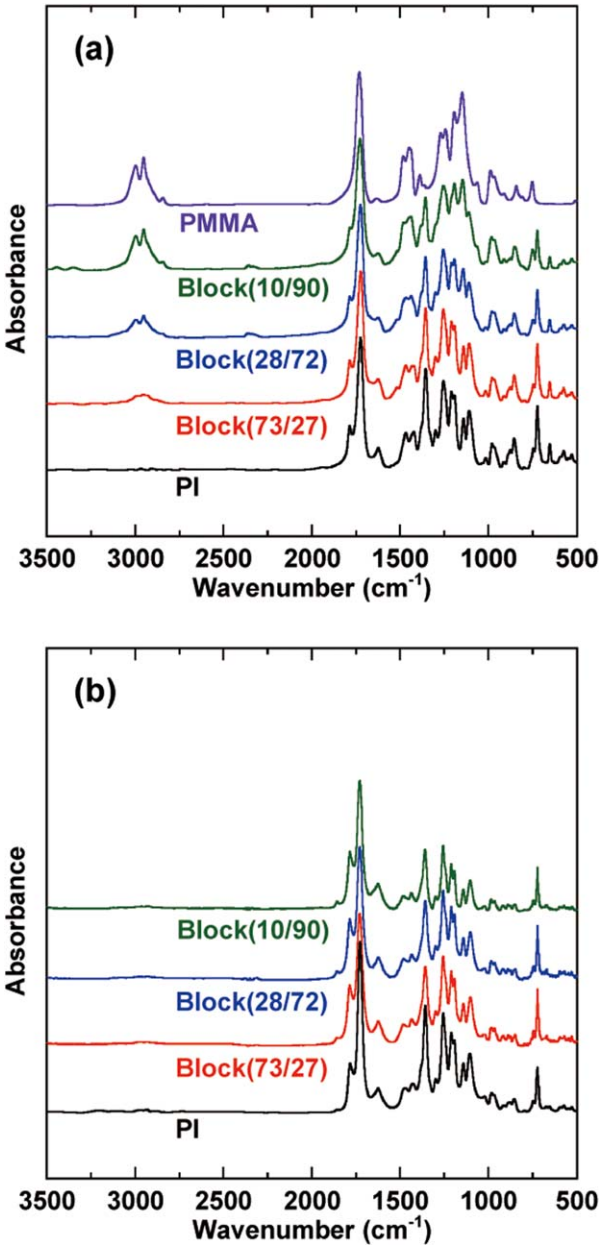

Figure 5. FT-IR spectra of Block(PI/PMMA) (a) before thermal treatment and (b) after thermal treatment. [Color figure can be viewed in the online issue, which is available at wileyonlinelibrary.com.]

3000 (C—H stretching), 1440 (C—H and —CH_2— bending), 1380 (—CH_3 asymmetric stretching), 1256 (C—O stretching), and 1147 cm^{-1} (C═O bending) derived from the PMMA component also increased. However, the peaks at 1785 (C═O asymmetric stretching), 1357, 1192 (C—F and C—N stretching), and 724 cm^{-1} (C═O bending) decreased. The peaks derived from the PMMA structure on thermally treated films could not be observed and were similar to those of the PI structure after thermal treatment. These results revealed an additive property between the PMMA content and peak intensity derived from PMMA in Block(PI/PMMA). In addition, PMMA block was completely decomposed by thermal treatment in all content ratios. To analyze the detailed structure, we calculated the intensity of the differential FT-IR spectra of Block(PI/PMMA), thermally treated films, and 6FDA-TeMPD and then compared with the PMMA structure.

Figure 6(a) presents the differential spectra intensity of Block(PI/PMMA) and 6FDA-TeMPD. The peak around 3000 cm^{-1} (C—H stretching) derived from PMMA increased with increasing PMMA content. The peaks at 1725 (C═O stretching), 1440 (C—H and —CH_2— bending), 1256 (C—O stretching), and 1147 cm^{-1} (C═O bending) derived from PMMA also increased. However, the peaks at 1357 cm^{-1} (C—F

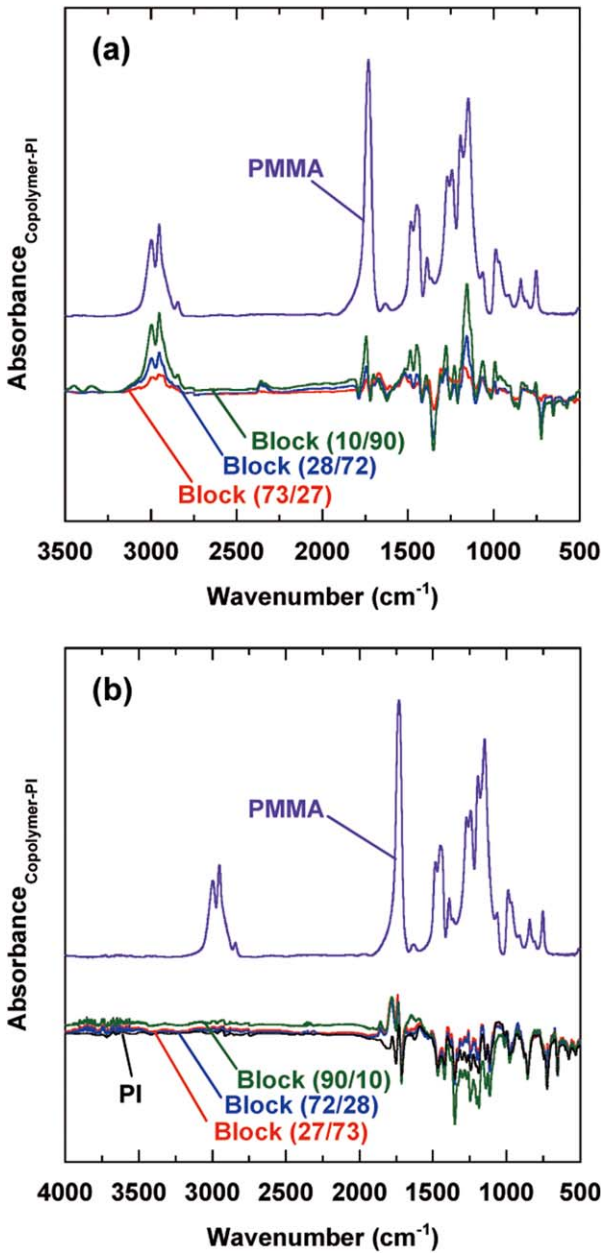

Figure 6. FT-IR differential spectra (a) between Block(PI/PMMA) and 6FDA-TeMPD before thermal treatment and (b) between each polymer after thermal treatment and before thermal treatment. [Color figure can be viewed in the online issue, which is available at wileyonlinelibrary.com.]

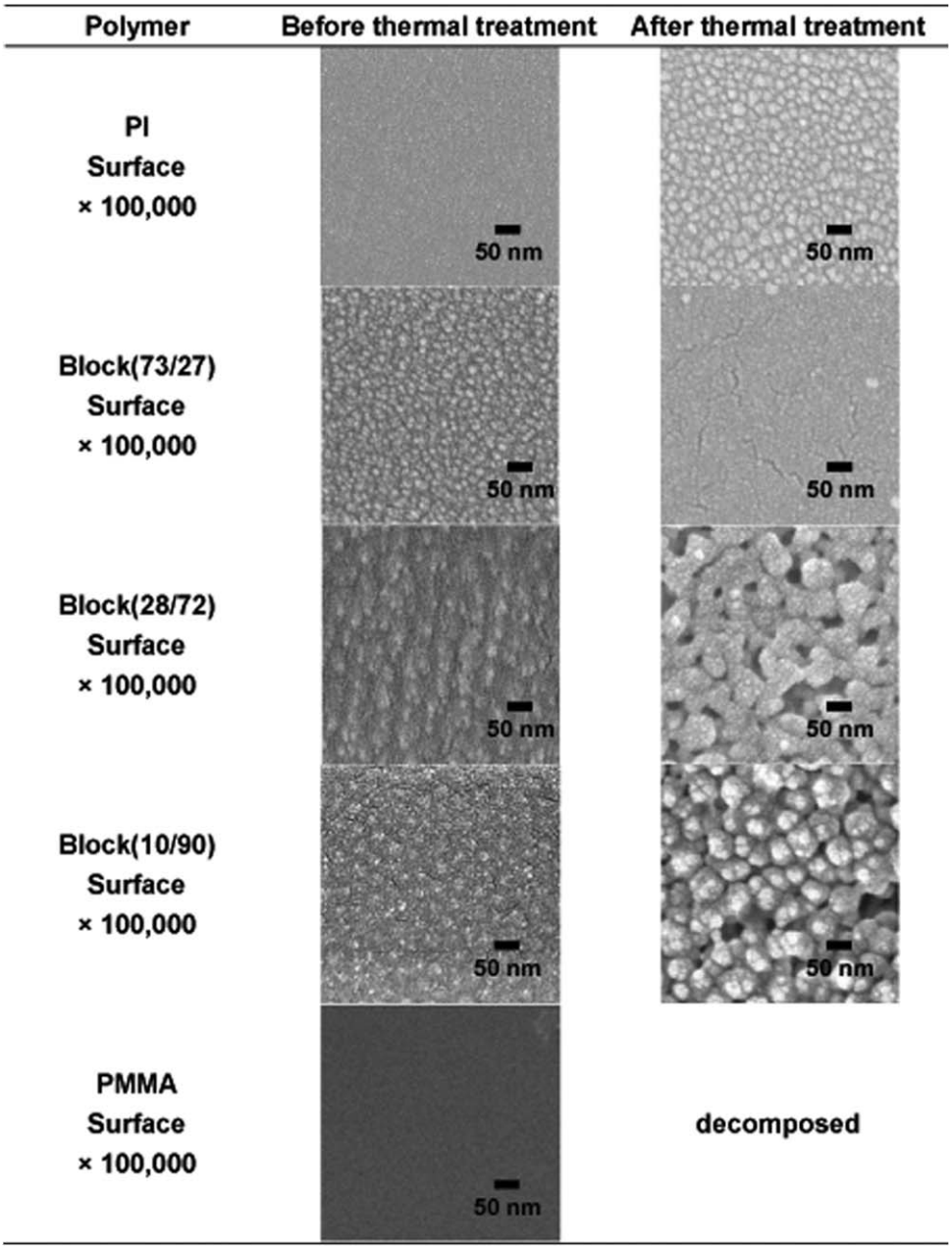

Figure 7. SEM images of Block(PI/PMMA) films.

and C—N stretching) derived from 6FDA-TeMPD and the peak (C═O bending) derived from imide ring decreased. The peaks derived from PMMA and PI increased with increasing PMMA content rate of triblock copolymer. Figure 6(b) presents the differential spectra intensity of thermally treated films and 6FDA-TeMPD. The peak of the stretching vibration around 3000 cm^{-1} derived from PMMA and the positive differential peaks were not observed in all films. Therefore, PMMA block completely decomposed. In addition, the peaks at 1500 (C—H bending), 1357, 1192 (C—F and C—N stretching), 1112 (C—F stretching), and 724 cm^{-1} (C═O bending) derived from 6FDA-TeMPD decreased in the differential peaks of thermally treated films and 6FDA-TeMPD. Block(PI/PMMA) was further observed in functional groups similar to that of 6FDA-TeMPD after thermal treatment. The differential peak of Block(10/90) was the maximum. These results indicated that the different structures on 6FDA-TeMPD block before and after thermal treatment resulted from the decomposition of their functional groups and/or the bond parts with PMMA block. Hence, decomposition of the 6FDA-TeMPD end chains was promoted in Block(10/90) because the long-length chain of PMMA easily promoted the movement of the 6FDA-TeMPD chains.

Figure 7 presents the SEM images of each polymer before and after thermal treatment. Surface image of Block(10/90) is citation of the previous study.[30] The flat and smooth surface structures were observed before thermal treatment of PMMA and 6FDA-TeMPD films. Surface asperity was observed in

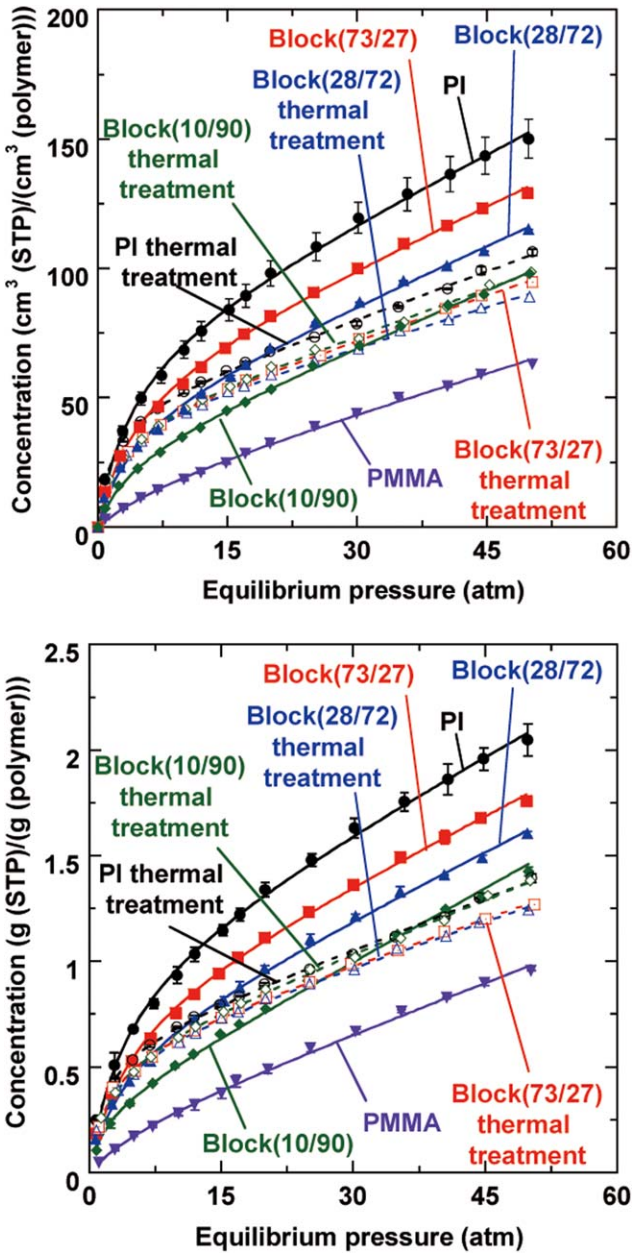

Figure 8. Sorption isotherms for CO_2 at 35°C in Block(PI/PMMA) films. The solid lines represent values before thermal treatment, whereas dotted lines demonstrate values after thermal treatment. [Color figure can be viewed in the online issue, which is available at wileyonlinelibrary.com.]

Block(PI/PMMA) films. This asperity was micro-phase separation caused by the PMMA block content rate. Block(10/90) presented a sea-island structure, whereas Block(73/27) and Block(28/72) exhibited inhomogeneous structures. Evident changes were also detected after thermal treatment of Block(PI/PMMA) films. The surface of Block(73/27) was flat, partially-clacked, and without phase-separation structure. Numerous pores with size of approximately 10–50 nm were observed in Block(28/72) and Block(10/90). Before thermal treatment, the clearest thermal transformation was observed in 10/90 block through DSC measurement; this block also demonstrated clearer microphase separation than the other block copolymers. After thermal treatment, shrinkage and surface structure analyses showed that lower than 27 mol % of the decomposed PMMA block did not affect the film structure of 6FDA-TeMPD. About 90 mol % of the decomposed PMMA block significantly influenced the film structure of 6FDA-TeMPD and formed dense structure through shrinkage. About 72 mol % of the decomposed PMMA block affected the film structure of 6FDA-TeMPD and minimized the shrinkage of the film. Therefore, Block(28/72) demonstrated the optimum balance pore and PI structure.

CO_2 Sorption Before Thermal Treatment

Gravimetric method showed that the CO_2 sorption isotherm in each polymer film at 35°C with PMMA varied from 0 atm to 50 atm; the results were compared and are presented in Figure 8. These isotherms fitted a dual-mode sorption model in all polymer films. This model can be expressed by[31]

$$C = C_D + C_H = k_D p + \frac{C'_H bp}{1+bp} \quad (1)$$

where C_D and C_H are the gas concentrations based on Henry's law sorption and Langmuir sorption, respectively. The parameter k_D is Henry's low coefficient, p is the gas pressure, and b and C'_H are the Langmuir hole affinity parameter and capacity parameter, respectively. The value of C'_H is related to the non-equilibrium excess free volume in a glassy polymer and described as follows:[31,32]

$$C'_H = \left(\frac{V_g - V_l}{V_g}\right)\rho^* \quad (2)$$

where V_g and V_l are the polymer specific volume (cm^3/g) in the glassy and hypothetical rubbery states, respectively. ρ^* is the molar density (mol/cm^3) of the penetrant in the Langmuir sites. The ρ^* value of carbon dioxide at 35°C is 0.0182 mol/cm^3.[33,34]

The dual-mode parameters obtained from a non-liner least-square regression analysis of the CO_2 sorption data in Figure 8 are summarized in Tables II and III. The order of CO_2 concentration was PI > Block(73/27) > Block(28/72) > Block(10/90) > PMMA under all pressure conditions, and CO_2 concentration decreased with increasing PMMA content. In thermally treated films, the order of CO_2 concentration was PI > Block(73/27) = Block(28/72) = Block(10/90) under all pressure conditions; these values were similar to the CO_2 concentration of Block(PI/PMMA) regardless of the PMMA content. These results suggested that the primary structure was similar to the structure of the decomposed PMMA block. SEM results after thermal treatment demonstrated a large difference in the surface structure of each film; however, the film structure did not influence the CO_2 concentration.

Figure 9 presents the differences (α) in the experimental values of CO_2 concentration and the theoretical values of CO_2 concentration calculated from content ratio in Block(PI/PMMA). α was expressed by[35]

$$\alpha = \frac{C_{\text{Copolymer}} - C_{\text{PI+PMMA}}}{C_{\text{Copolymer}}} \quad (3)$$

where $C_{\text{PI+PMMA}}$ is the sum of the CO_2 concentration of PI homopolymer × PI content ratio in Block(PI/PMMA) and the CO_2 concentration of PMMA homopolymer × PMMA content

Table II. Dual-Mode Sorption Parameters for CO_2 in 6FDA-TeMPD (PI), PMMA, and Block(PI/PMMA) Before Thermal Treatment

Polymer	ρ[a] (g/cm^3)	k_D (cm^3(STP)/(cm^3(polymer)atm))	C'_H (cm^3(STP)/cm^3(polymer))	b (1/atm)	S_0 (cm^3(STP)/(cm^3(polymer)))	S_{H0}/S_0	C'_H/ρ^*
PI	1.333 ± 0.001	1.66 ± 0.06	75.7 ± 1.4	0.246 ± 0.005	20.3 ± 0.8	0.92 ± 0.01	0.183 ± 0.021
Block (73/27)	1.337 ± 0.001	1.50 ± 0.09	62.1 ± 5.0	0.225 ± 0.037	15.3 ± 1.2	0.90 ± 0.01	0.152 ± 0.017
Block (28/72)	1.304 ± 0.001	1.46 ± 0.03	46.8 ± 0.5	0.241 ± 0.022	12.7 ± 0.9	0.88 ± 0.01	0.115 ± 0.002
Block (10/90)	1.251 ± 0.001	1.42 ± 0.08	30.1 ± 2.3	0.250 ± 0.039	8.9 ± 0.7	0.84 ± 0.01	0.074 ± 0.008
PMMA	1.199 ± 0.003	0.79 ± 0.15	35.1 ± 11.4	0.046 ± 0.007	2.33 ± 0.1	0.66 ± 0.08	0.086 ± 0.039

[a] Cited from Ref. 29.

Table III. Dual-Mode Sorption Parameters for CO_2 in 6FDA-TeMPD (PI) and Block(PI/PMMA) After Thermal Treatment

Polymer	ρ (g/cm^3)	k_D (cm^3(STP)/(cm^3(polymer)atm))	C'_H (cm^3(STP)/cm^3(polymer))	b (1/atm)	S_0 (cm^3(STP)/(cm^3(polymer)))	S_{H0}/S_0	C'_H/ρ^*
PI thermally treated	1.388 ± 0.014	1.20 ± 0.01	46.4 ± 0.4	0.628 ± 0.017	30.4 ± 1.0	0.96 ± 0.01	0.114 ± 0.001
Block (73/27) thermally treated	1.400 ± 0.001	1.11 ± 0.09	41.2 ± 0.7	0.476 ± 0.002	20.7 ± 0.2	0.95 ± 0.01	0.101 ± 0.002
Block (28/72) thermally treated	1.304 ± 0.001	0.99 ± 0.07	42.6 ± 0.5	0.418 ± 0.009	18.8 ± 0.6	0.95 ± 0.01	0.105 ± 0.001
Block (10/90) thermally treated	1.300 ± 0.001	1.17 ± 0.11	41.3 ± 1.2	0.444 ± 0.011	19.5 ± 0.3	0.94 ± 0.01	0.101 ± 0.003

ratio in Block(PI/PMMA) $C_{Copolymer}$ is the CO_2 concentration of Block(PI/PMMA). The experimental values of Block(PI/PMMA) were lower than the theoretical values. For the concentration of Block(PI/PMMA), the experimental values were approximately 20% to 30% lower than the theoretical value in the low-pressure region at 0 atm and about 0% to 15% lower than the theoretical value in the high-pressure region at 50 atm. As demonstrated in the fluorescence spectra measurement in previous study, the formation of charge-transfer complex (CTC) of PI block affected the CO_2 concentration of Block(PI/PMMA). Previous study[29] reported that the PMMA segment of Block(PI/PMMA) increased the charge-transfer (CT) effect of PI; triblock copolymer with shorter PMMA block was significantly influenced compared with the polymer with longer PMMA block. Therefore, the CT effect corresponded to that of α. For the decreased concentration caused by the CT effect, the experimental concentration was lower than the theoretical concentration.

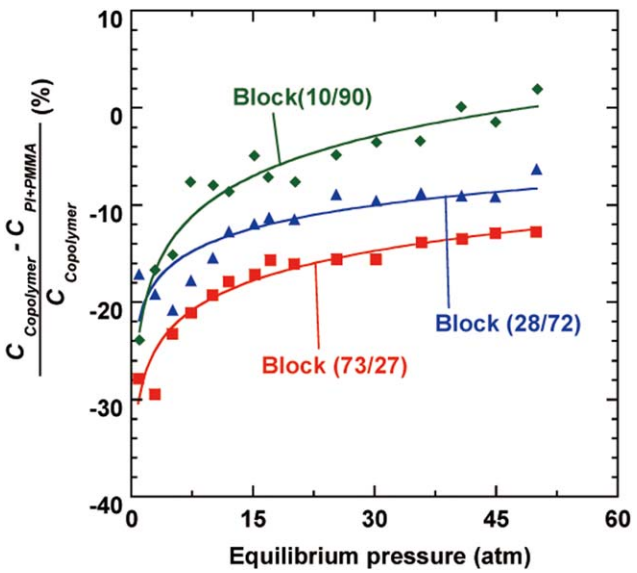

Figure 9. Ratio of the CO_2 concentration relationship between theoretical and experimental values of Block(PI/PMMA) films. [Color figure can be viewed in the online issue, which is available at wileyonlinelibrary.com.]

Figure 10 presents the differences (β) in CO_2 concentration before and after thermal treatment. β was expressed by

$$\beta = \frac{C_{\text{After thermal treatment}} - C_{\text{Before thermal treatment}}}{C_{\text{After thermal treatment}}} \quad (4)$$

The CO_2 concentrations of PI decreased in all pressure regions. The CO_2 concentration in PI films was decreased by thermal treatment as indicated by the increasing CT effect.[8] Therefore, the concentration of PI decreased because the formation of CTC was promoted by thermal treatment. The concentration of

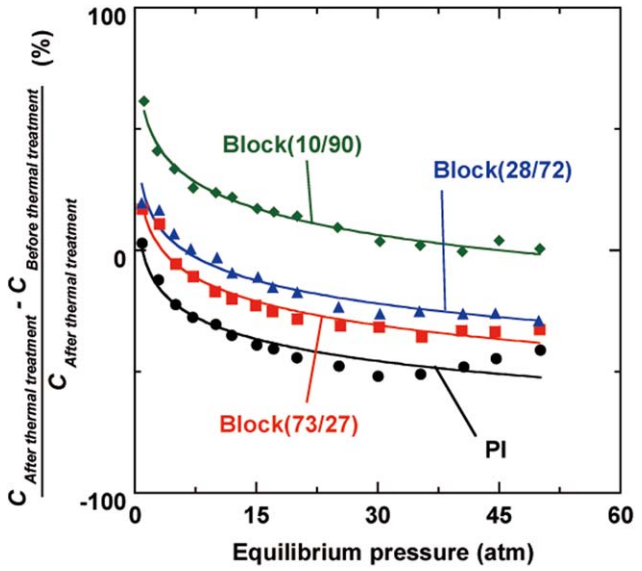

Figure 10. Ratio of CO_2 concentration before thermal treatment of Block(PI/PMMA) films to that after thermal treatment. [Color figure can be viewed in the online issue, which is available at wileyonlinelibrary.com.]

Block(73/27) and Block(28/72) increased by about 20% in low-pressure region (<2 atm) and decreased by about 30% in high-pressure region (>49 atm) compared with non-treated films. The CO_2 concentration of thermally treated films decreased with increasing pressure compared with nontreated films. The concentration of Block(10/90) increased by about 60% in low-pressure region (<2 atm) and decreased by less than 1% in high-pressure region (>49 atm) compared with those of the nontreated films. The difference in CO_2 concentration of thermally treated films increased with increasing PMMA block content.

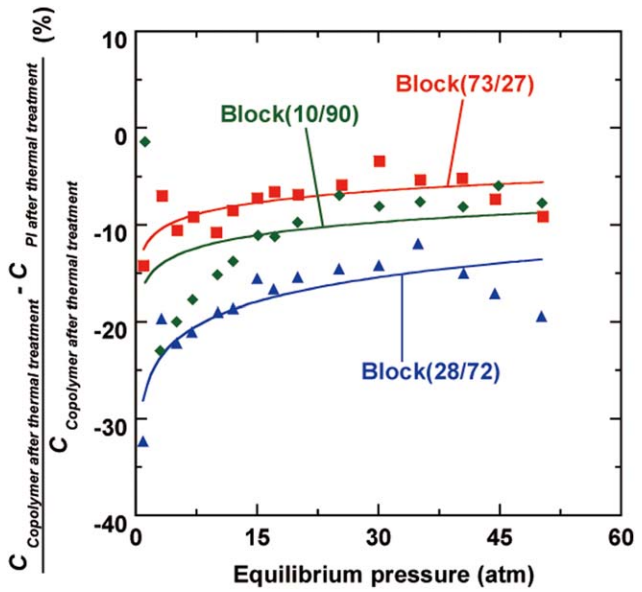

Figure 11. Ratio of the CO_2 concentration relationship between PI and copolymers after thermal treatment of Block(PI/PMMA) films. [Color figure can be viewed in the online issue, which is available at wileyonlinelibrary.com.]

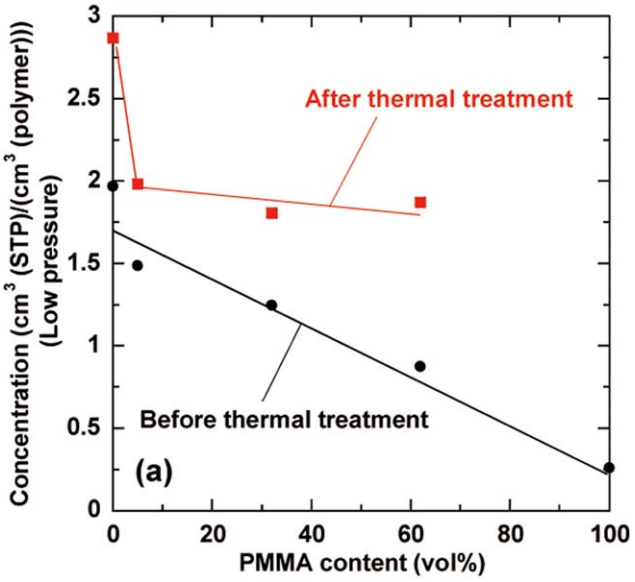

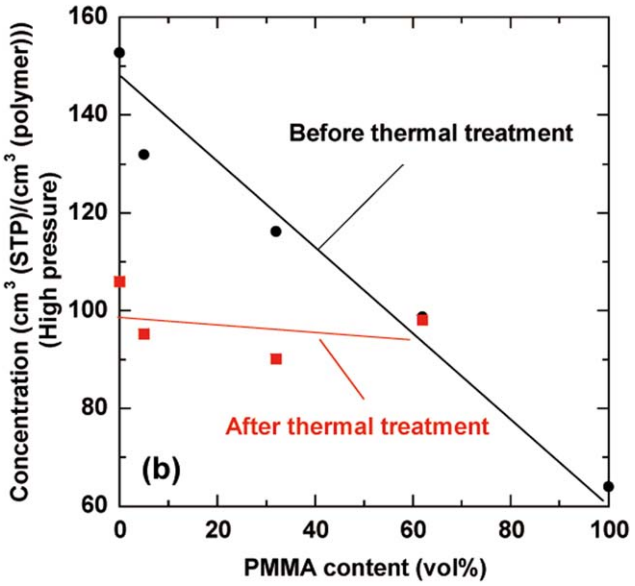

Figure 12. CO_2 concentration of Block(PI/PMMA) films as a function of its PMMA content in the (a) low-pressure region and (b) high-pressure region. [Color figure can be viewed in the online issue, which is available at wileyonlinelibrary.com.]

Figure 11 demonstrates the differences (γ) in CO_2 concentration before and after thermal treatment. γ was expressed by

$$\gamma = \frac{C_{\text{Cpolymer after thermal treatment}} - C_{\text{PI after thermal treatment}}}{C_{\text{Copolymer after thermal treatment}}} \quad (5)$$

The order of CO_2 concentration was Block(73/27) > Block(10/90) > Block(28/72) and the CO_2 concentration of Block(PI/PMMA) was lower than that of PI. Therefore, the content ratio of PMMA block in triblock copolymers did not directly influence the concentration during thermal treatment.

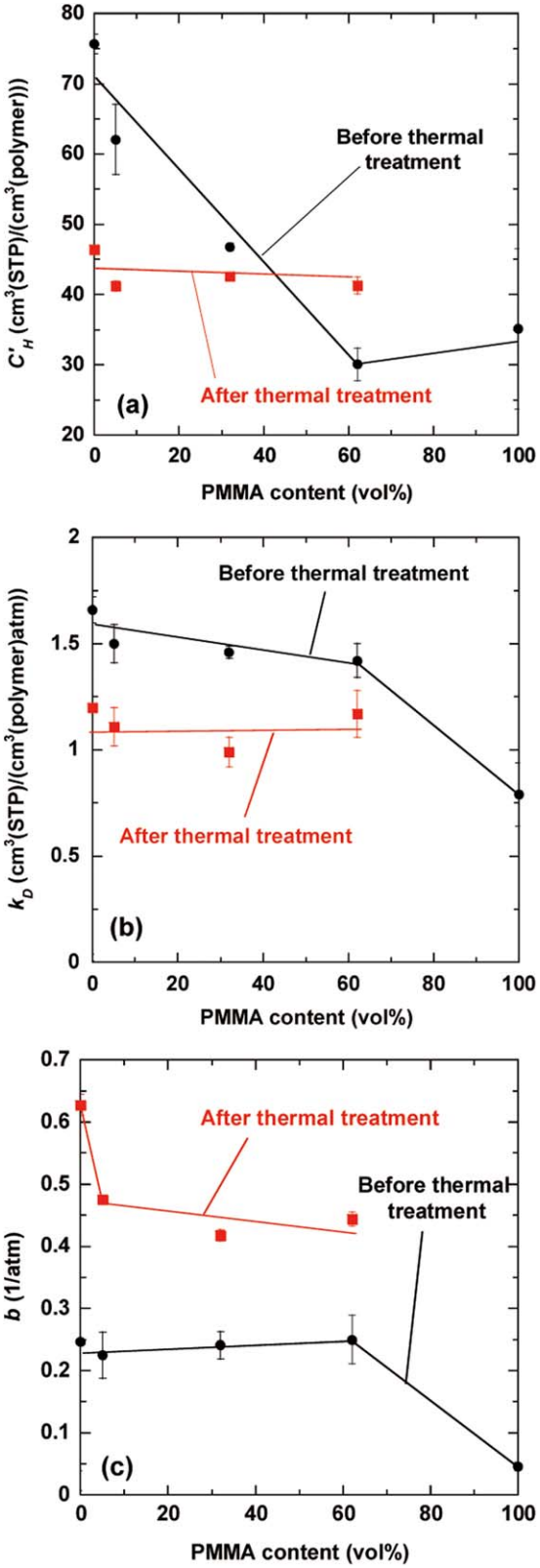

Figure 13. Dual-mode sorption parameters of Block(PI/PMMA) films as a function of its PMMA content. (a) Henry's law constant (k_D), (b) Langmuir capacity constant (C'_H), and (c) hole affinity constant (b). [Color figure can be viewed in the online issue, which is available at wileyonlinelibrary.com.]

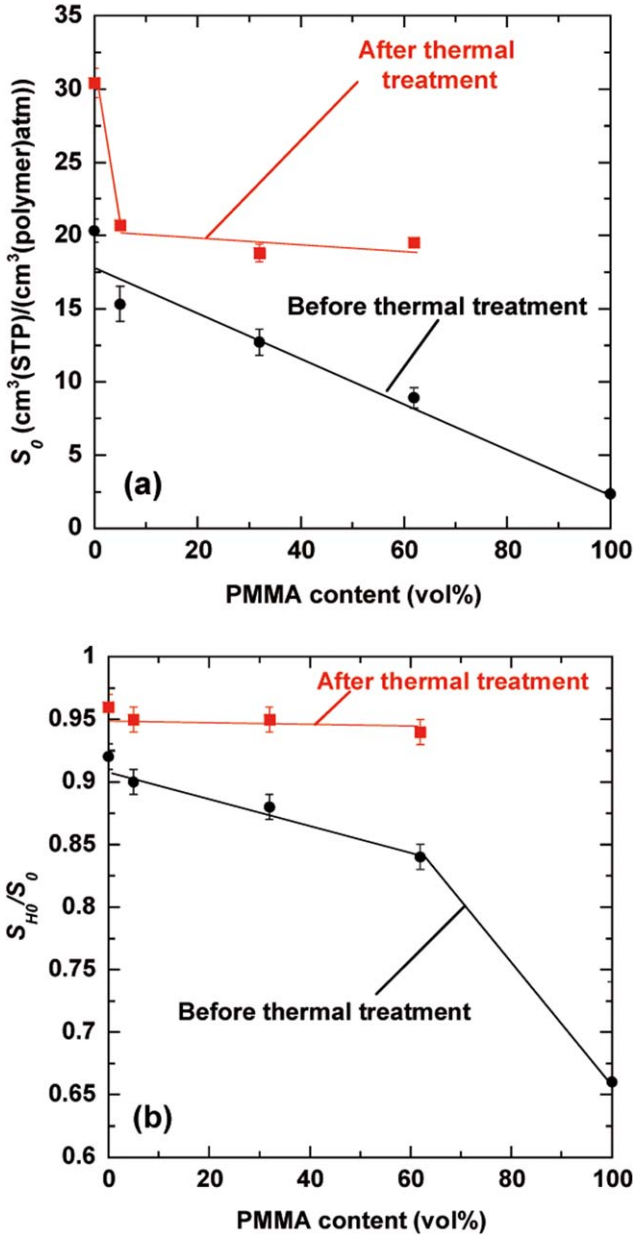

Figure 14. Infinite-dilution CO_2 solubility at 35°C in Block(PI/PMMA) films as a function of its PMMA content. (a) Infinite-dilution solubility and (b) the Langmuir-type contribution solubility at infinite dilution. [Color figure can be viewed in the online issue, which is available at wileyonlinelibrary.com.]

Figure 12 shows the CO_2 concentration of Block(PI/PMMA) films as a function of their PMMA contents in the low- and high-pressure regions. The order of CO_2 concentration was Block(73/27) > Block(10/90) > Block(28/72) in the low- and high-pressure regions. Thus, the concentration and PMMA content ratio were directly related. The CO_2 concentration of thermally treated films showed a constant value regardless of the PMMA content in the low- and high-pressure regions. Interestingly, the CO_2 concentration of thermally treated films in the low-pressure region was higher than that in the high-pressure

region. Therefore, CO_2 concentration increased in Langmuir's region but decreased in Henry's region in all thermally treated films compared with that in the untreated films.

The parameters k_D, C'_H, and b of the polymer films at 35°C as a function of the PMMA content in each polymer are shown in Figure 13. C'_H of PI was 2.2 times higher than that of PMMA. A linear relationship could not be obtained in triblock copolymers. The order of C'_H was PI > Block(73/27) > Block(28/72) > PMMA > Block(10/90). Thus, the free volume in the films was influenced by the micro-phase separation structure. k_D and b in all polymers were similar except for PMMA and PMMA, which were 50% lower than those of the other polymers. b and CO_2 concentration in Henry's region of Block(PI/PMMA) depended on the PI structure, whereas C'_H of Block(PI/PMMA) depended on the microphase separation structure of triblock copolymers. These parameters were similar to those of thermally treated films, regardless of PMMA content; however, b of thermally treated PI films was 30% higher than that of thermally treated Block(PI/PMMA).

The solubility of a gas molecule in glassy polymers can be expressed by the dual-mode sorption parameter:[31,32,36]

$$S \equiv \frac{C}{p} = S_D + S_H = k_D + \frac{C'_H b}{1+bp} \quad (6)$$

where S is the solubility of the penetrant, S_D and S_H are the solubility values based on Henry's low and Langmuir-type sorption, respectively.

The infinite-dilution solubility S_0 is given by:[31,32]

$$S_0 = \lim_{p\to 0}\left(\frac{C}{p}\right) \approx S_{D0} + S_{H0} = k_D + C'_H b \quad (7)$$

where S_{D0} and S_{H0} are the solubility values in the Henry's law and Langmuir sorption regions at infinite-dilution, respectively. The S_0 and S_{H0} values estimated from eq. (7) using the dual-mode sorption parameters are summarized in Tables II and III.

Figure 14 presents the infinite-dilution CO_2 solubility at 35°C in Block(PI/PMMA) films as a function of PMMA content. The order of S_0 values was PI > Block(73/27) > Block(28/72) > Block(10/90) > PMMA. As the PMMA content increased, the S_0 values decreased. However, the order of S_{H0}/S_0 value in non-treated films was PI > Block(73/27) > Block(28/72) > Block(10/90) >> PMMA. Interestingly, S_{H0}/S_0 in each polymer varied from 0.84 to 0.92. This result indicated that the total infinite-dilution solubility values of CO_2 were equivalent to those in the Langmuir sites. The order of S_0 value in thermally treated films was PI > Block(73/27) ≈ Block(28/72) ≈ Block(10/90). S_0 of thermally treated Block(PI/PMMA) was similar to that of triblock copolymer, regardless of PMMA content. However, S_0 of PI was about 50% higher than that of each thermally treated Block(PI/PMMA) regardless of their similar thermal-treated Block(PI/PMMA) structure. The order of S_{H0}/S_0 value in thermally treated films was PI ≈ Block(73/27) ≈ Block(28/72) ≈ Block(10/90). S_{H0}/S_0 in each polymer varied from 0.94 to 0.96. This result indicated that the total infinite-dilution solubility values of CO_2 were almost equivalent in the Langmuir sites but higher than those in nontreated films.

CONCLUSION

We investigated the effects of PMMA content and thermal treatment on CO_2 sorption of ABA-type triblock copolymers derived from PI and PMMA. TGA results showed that thermally labile blocks in Block(PI/PMMA) can be completely decomposed under a thermal condition presented in previous study.[7] SEM results demonstrated that the asperity was microphase separation caused by the PMMA block content rate. Numerous pores with sizes of approximately 10 to 50 nm were observed in the Block(28/72) and Block(10/90). The isotherms fitted the dual-mode sorption model in all polymer films, and CO_2 sorption decreased with increasing PMMA content rate. Infinite-dilution CO_2 solubility depended on Langmuir's site of each polymer because S_{H0}/S_0 of PI and Block(PI/PMMA) varied from 0.84 to 0.92. CO_2 affinity was increased by thermal treatment as indicated by the higher b and S_0 values of thermally treated films than that of the nontreated films.

ACKNOWLEDGMENTS

This research was partially supported by a Grant-in-aid for Scientific Research C (24560862) from the Ministry of Education, Culture, Sports, Science and Technology, Japan, the Japanese Society of the Promotion of Science and Research Project Grant B (3) from the Institute of Science and Technology, Meiji University, Japan.

REFERENCES

1. Yang, C.-P.; Su, Y.-Y. *Polymer* **2005**, *46*, 5797.
2. Creed, D.; Hoyle, C. E.; Subramanian, P.; Nagarajan, R.; Pandey, C.; Anzures, E. T.; Cane, K. M.; Cassidy, P. E. *Macromolecules* **1994**, *27*, 832.
3. Hoyle, C. E.; Anzures, E. T.; Subramanian, P.; Nagarajan, R.; Creed, D. *Macromolecules* **1992**, *25*, 6651.
4. Srisuwan, S.; Thongyai, S.; Praserthdam, P. *J. Appl. Polym. Sci.* **2010**, *117*, 2422.
5. Miyata, S.; Sato, S.; Nagai, K.; Nakagawa, T.; Kudo, K. *J. Appl. Polym. Sci.* **2008**, *107*, 3933.
6. Sato, S.; Ose, T.; Miyata, S.; Kanehashi, S.; Ito, H.; Matsumoto, S.; Iwai, Y.; Matsumoto, H.; Nagai, K. *J. Appl. Polym. Sci.* **2011**, *121*, 2794.
7. Miyata, S.; Shirokura, H.; Nagai, K. *Kobunshi Ronbunshu* **2009**, *66*, 170.
8. Kanehashi, S.; Sato, S.; Nagai, K. *Polym. Eng. Sci.* **2011**, *51*, 2360.
9. Sato, S.; Gondo, D.; Sugiyama, H.; Nagai, K.; Matsumoto, S.; Matsumoto, H. *J. Photopolym. Sci. Technol.* **2012**, *25*, 401.
10. Sato, S.; Ito, H.; Mizunuma, T.; Nagai, K.; Matsumoto, H.; Matsumoto, S. *J. Photopolym. Sci. Technol.* **2011**, *24*, 617.
11. Nakamura, K.; Kitagawa, T.; Nara, S.; Wakamatsu, T.; Ishiba, Y.; Kanehashi, S.; Sato, S.; Nagai, K. *Ind. Eng. Chem. Res.* **2013**, *52*, 1133.
12. Kanehashi, S.; Onda, M.; Shindo, R.; Sato, S.; Kazama, S.; Nagai, K. *Polym. Eng. Sci.* **2013**, *53*, 1667.
13. Sato, S.; Suzuki, M.; Kanehashi, S.; Nagai, K. *J. Membr. Sci.* **2010**, *360*, 352.

14. Kanehashi, S.; Gu, H.; Shindo, R.; Sato, S.; Miyakoshi, T.; Nagai, K. *J. Appl. Polym. Sci.* **2013**, *128*, 3814.
15. Kanehashi, S.; Nakagawa, T.; Nagai, K.; Duthie, X.; Kentish, S.; Stevens, G. *J. Membr. Sci.* **2007**, *298*, 147.
16. Scholes, C. A.; Ribeiro, C. P.; Kentish, S. E.; Freeman, B. D. *J. Membr. Sci.* **2014**, *450*, 72.
17. Calle, M.; Doherty, C. M.; Hill, A. J.; Lee, Y. M. *Macromolecules* **2013**, *46*, 8179.
18. Guo, R.; Sanders, D. F.; Smith, Z. P.; Freeman, B. D.; Paul, D. R.; McGrath, J. E. *J. Mater. Chem. A* **2013**, *1*, 6063.
19. Smith, Z. P.; Sanders, D. F.; Ribeiro, C. P.; Guo, R.; Freeman, B. D.; Paul, D. R.; McGrath, J. E.; Swinnea, S. *J. Membr. Sci.* **2012**, *415*, 558.
20. Kim, S.; Woo, K. T.; Lee, J. M.; Quay, J. R.; Murphy, M. K.; Lee, Y. M. *J. Membr. Sci.* **2014**, *453*, 556.
21. Kostina, J.; Rusakova, O.; Bondarenko, G.; Alentiev, A.; Meleshko, T.; Kukarkina, N.; Yakimanskii, A.; Yampolskii, Y. *Ind. Eng. Chem. Res.* **2013**, *52*, 10476.
22. Nguyen, T. H.; Wang, C.; Wang, X. *J. Membr. Sci.* **2009**, *342*, 208.
23. Choi, J.; Takayama, T.; Yu, H.-C.; Chung, C.-M.; Kudo, K. *Polymer* **2012**, *53*, 1328.
24. Hedrick, J. L.; Charlier, Y.; DiPietro, R.; Jayaraman, S.; McGrath, J. E. *J. Polym. Sci. Part A: Polym. Chem.* **1996**, *34*, 2867.
25. Fodor, J. S.; Briber, R. M.; Russell, T. P.; Carter, K. R.; Hedrick, J. L.; Miller, R. D. *J. Polym. Sci. Part B: Polym. Phys.* **1997**, *35*, 1067.
26. Hedrick, J. L.; Carter, K.; Sanchez, M.; Di Pietro, R.; Swanson, S.; Jayaraman, S.; McGrath, J. G. *Macromol. Chem. Phys.* **1997**, *198*, 549.
27. Miyata, S.; Yoshida, K.; Shirokura, H.; Kashio, M.; Nagai, K. *Polym. Int.* **2009**, *58*, 1148.
28. Miyata, S.; Nagai, K. *Chem. Lett.* **2007**, *36*, 1114.
29. Kanehashi, S.; Koyama, Y.; Ando, S.; Konishi, S.; Shindo, R.; Miyata, S.; Sato, S.; Miyakoshi, T.; Nagai, K. *Polym. Int.* **2014**, *63*, 435.
30. Sato, S.; Ichikawa, M.; Ose, T.; Miyata, S.; Takahashi, Y.; Kanehashi, S.; Matsumoto, H.; Nagai, K. *Polym. Int.* **2013**, *62*, 1377.
31. Kanehashi, S.; Nagai, K. *J. Membr. Sci.* **2005**, *253*, 117.
32. Nagai, K.; Kanehashi, S.; Tabei, S.; Nakagawa, T. *J. Membr. Sci.* **2005**, *251*, 101.
33. Li, G. Z.; Cho, H.; Wang, L.; Toghiani, H.; Pittman, C. U. *J. Polym. Sci. Part A: Polym. Chem.* **2005**, *43*, 355.
34. Prausnitz, J. M.; Shair, F. H. *AIChE J.* **1961**, *7*, 682.
35. Nagai, K. *Kobunshi Ronbunshu* **2003**, *60*, 482.
36. Kanehashi, S.; Nakagawa, T.; Nagai, K.; Duthie, X.; Kentish, S.; Stevens, G. *J. Membr. Sci.* **2007**, *298*, 147.